MRI-TRUS Image Synthesis with Application to Image-Guided Prostate Intervention

John A. Onofrey[1], Ilkay Oksuz[1,4], Saradwata Sarkar[5], Rajesh Venkataraman[5], Lawrence H. Staib[1,2,3], and Xenophon Papademetris[1,2]

[1] Departments of Radiology & Biomedical Imaging
[2] Biomedical Engineering
[3] Electrical Engineering
Yale University, New Haven, CT 06520, USA,
[4] IMT Institute for Advanced Studies Lucca, Italy
[5] Eigen, Grass Valley, CA 95945, USA,
{john.onofrey,ilkay.oksuz,lawrence.staib,xenophon.papademetris}@yale.edu,
{sarad.sarkar,rajesh.venkataraman}@eigen.com

Abstract. Accurate and robust fusion of pre-procedure magnetic resonance imaging (MRI) to intra-procedure trans-rectal ultrasound (TRUS) imaging is necessary for image-guided prostate cancer biopsy procedures. The current clinical standard for image fusion relies on non-rigid surface-based registration between semi-automatically segmented prostate surfaces in both the MRI and TRUS. This surface-based registration method does not take advantage of internal anatomical prostate structures, which have the potential to provide useful information for image registration. However, non-rigid, multi-modal intensity-based MRI-TRUS registration is challenging due to highly non-linear intensities relationships between MRI and TRUS. In this paper, we present preliminary work using image synthesis to cast this problem into a mono-modal registration task by using a large database of over 100 clinical MRI-TRUS image pairs to learn a joint model of MR-TRUS appearance. Thus, given an MRI, we use this learned joint appearance model to synthesize the patient's corresponding TRUS image appearance with which we could potentially perform mono-modal intensity-based registration. We present preliminary results of this approach.

1 Introduction

Non-rigid registration of multi-modal images is a challenging problem for image-guided interventions. The highly non-linear intensity relationships between such multi-modal images and the high dimensionality of the non-rigid deformation make registration optimization difficult. In contrast to intensity-based registration, image segmentation offers an alternative strategy to register images where corresponding structures in both image are first segmented and then these segmented structures are subsequently registered to each other. However, image segmentation, both automated and manual, is itself a difficult problem that is

prone to error and high variability. Furthermore, depending upon the segmentation's granularity, potentially useful information for the registration about the anatomy, *e.g.* fine internal anatomical structures within a volume of interest, could be abstracted away by the segmentation. In this paper, we present preliminary work to convert this multi-modal image registration task into a mono-modal registration task using image synthesis. Using a large set of manually-labeled, multi-modal training data, we learn a model of intensity appearance between two different modality images, and then use this model to synthesize the appearance of a target image given an image of the other modality. We present results applying our approach to synthesize trans-rectal ultrasound (TRUS) imaging from magnetic resonance imaging (MRI) for image-guided prostate biopsy localization.

With over 450,000 men estimated to be diagnosed with prostate cancer in the year 2015 [14], prostate cancer is one of the most commonly occurring forms of cancer and one of the major causes of cancer-related death in the U.S. TRUS image-guided biopsy is the current clinical standard for diagnosing prostate cancer. The biopsy sampling procedure consists of two parts: *(i)* 12 untargeted, systematic tissue cores, in a non-patient-specific plan, from different regions of the prostate; and *(ii)* a small number of TRUS-guided targeted biopsies. While TRUS itself cannot be reliably used for targeting suspicious lesions because of poor image quality and lack of contrast, multi-parametric MRI (mpMRI) that combines T2-weighted imaging with functional sequences, *e.g.* diffusion-weighted MRI, spectroscopic MRI and dynamic contrast enhanced MRI, shows significantly better localization of suspicious lesions within the prostate [2]. To avoid performing biopsies under MRI guidance, which can be time consuming, expensive and impractical [15], current practice aims to fuse pre-procedure mpMRI with intra-procedure TRUS imaging. In this case, clinicians identify suspicious prostatic tissue using mpMRI and then urologists use TRUS imaging to provide targeted image-guided navigation for biopsy. Rigid registration between the MRI and TRUS is inadequate for accurate biopsy guidance due to prostate gland deformations caused by *(i)* variations in patient orientation, *(ii)* changes in bladder or rectal filling, *(iii)* and presence or absence of an endorectal MR coil, and *(iv)* deformation caused by handheld TRUS probes. Therefore, non-rigid registration is required to accurately compensate for these deformations.

A variety of non-rigid registration methods have been proposed to fuse MR and TRUS images for prostate biopsy. Previously proposed surface registration algorithms to align the segmented prostate surfaces from the MRI and TRUS images [9, 8] are highly operator dependent because they rely upon semi-automated segmentation methods, which are both time-consuming and prone to significant variability. As an alternative to surface-based registration, Sparks *et al.* [12] perform image fusion by first performing a probabilistic segmentation of the prostate in TRUS images, and then register this segmentation probability map. Karnik *et al.* [6] suggest that intensity-based registration methods may perform better than surface-based registration methods, and have the additional benefit that they do not require segmentation. Mitra *et al.* [7] propose an

intensity-based registration method, but validated it only on mid-gland MRI-TRUS slices. Rather than using raw intensity values, Sun *et al.* [13] propose MRI-TRUS fusion using an intensity-based non-local feature descriptor, but this strategy relies on analogous structures existing in both image volumes, which does not necessarily hold in the poor quality TRUS images. Some other works have used mono-modal TRUS image registration to perform intra-operative updates of the guidance. Xu *et al.* [17] use a combination of image intensity and image intensity gradient information to register 2D TRUS image slices to a 3D TRUS reference volume. Xu *et al.* [16] use mono-modal TRUS registration to perform updates during the biopsy procedure, but their method makes the assumption that the initial pre-operative TRUS acquisition aligns well with the MRI.

Similar to these works, we seek to perform non-rigid mono-modal TRUS image registration to update the image-guided biopsy procedure. In this work, we present a method to synthesize the TRUS image appearance for a given MRI. Rather than adopting a synthesis methodology that models the physics of image acquisition [5, 4], in this work we attempt to learn the appearance relationship of one modality from another based on a large set of richly-annotated, clinical MRI-TRUS training data. Our method, described in Sec. 2, builds a subject-specific joint MRI-TRUS appearance model by first warping all MRI-TRUS image pairs into the space of the test MRI. In this paper, we test two different methods to build this model: *(i)* using a principal component analysis (PCA)-based approach; and *(ii)* using a dictionary learning approach. We then use these learned models of appearance to synthesize a novel TRUS image that corresponds to the patients pre-procedure MRI. Our preliminary results, in Sec. 3 demonstrate approaches to synthesize qualitatively realistic TRUS images given an MRI.

2 Methods

Sec. 2.1 begins by describing the pre-processing steps necessary to create our database of training data. In Sec. 2.2, we detail our methods for jointly modeling MR-TRUS appearance, and how we apply this model to synthesize TRUS images given novel MRIs. Fig. 1 illustrates our method's model building and synthesis workflow.

2.1 MRI-TRUS Training Data and Pre-processing

We train our MRI-TRUS model of joint appearance using data from a clinical database of $N = 105$ patients undergoing prostate biopsy at our institution. For each patient, the dataset contains a pre-procedure T2-weighted MRI I_{MR}, an intra-procedure TRUS image I_{TRUS}, as well as segmented prostate surfaces S_{MR} and S_{TRUS} in each image. Both surfaces were generated using a semi-automated, clinical segmentation tool (Eigen, Grass Valley, CA). For each MRI-TRUS image pair, we account for deformations induced by the biopsy procedure by non-rigidly registering the TRUS image to the MRI space using a surface-based registration.

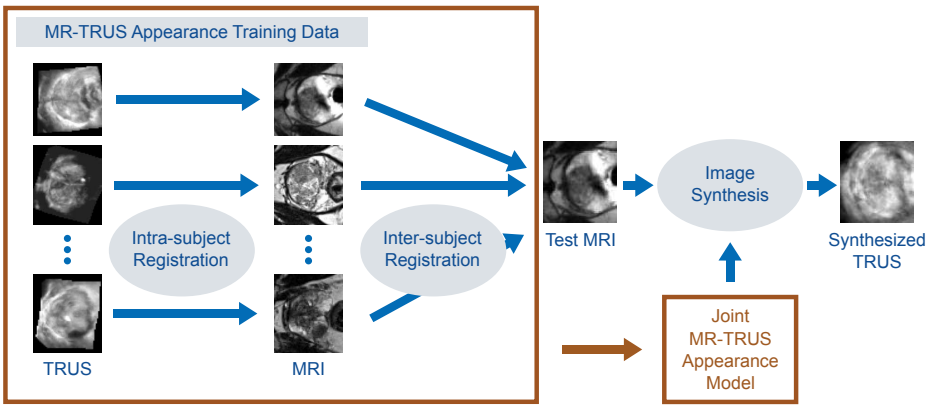

Fig. 1. Our workflow for training a patient-specific joint MRI-TRUS appearance model and synthesizing novel TRUS images. We make use of a large database of richly annotated data to learn a model of MRI-TRUS appearance. Given a novel, test MRI, we first warp all the MRI and TRUS images in our database to the test image's space using a series of intra-subject and inter-subject registrations. We then use these transformed image pairs as training data to learn the model of MRI-TRUS appearance. We then use this model to synthesize the corresponding TRUS image for that patient.

For each image $i = 1, \ldots, N$, we non-rigidly register $S_{\text{TRUS},i}$ to $S_{\text{MR},i}$ using a robust point matching (RPM) framework [3] with the transformation parameterized by a free-form deformation (FFD) [11, 10] with 10.0mm isotropic control point spacing; We denote these transformations $T_{\text{TRUS}\rightsquigarrow\text{MR}}$, where $i \rightsquigarrow j$ indicates nonrigid transformation from space i to j. We use all this data to create our patient-specific models of joint MRI-TRUS appearance as described in the next section.

2.2 Joint MR-TRUS Appearance Modeling

For a novel MRI I_{MR} not included in the training set, we warp our training data into this image's space. To do this, we perform N inter-subject MRI-MRI registrations. These registrations use a non-rigid RPM registration with 5.0 mm isotropic control point spacing [3, 10], and we denote these transformations $T_{\text{MR}\rightsquigarrow\text{MR},i}$ for $i = 1, \ldots, N$. Using these transformations and the intra-subject transformations from Sec. 2.1, we reslice all training images to the MRI reference space using the following:

$$I'_{\text{MR},i} = T_{\text{MR}\rightsquigarrow\text{MR},i} \circ I_{\text{MR},i}$$
$$I'_{\text{TRUS},i} = T_{\text{TRUS}\rightsquigarrow\text{MR},i} \circ T_{\text{MR}\rightsquigarrow\text{MR},i} \circ I_{\text{MR},i}$$

for all $i = 1, \ldots, N$ patients in the training database, where $\circ$ is the transformation operator.

With the N training images resliced to this common space, we construct our joint model of MRI-TRUS appearance. First, we center both the MRI and the

TRUS data to have the same median intensity inside the prostate, where the prostate is defined by the segmented surface S_{MR} for the test patient. Rather than modeling the appearance of the entire MRI reference volume $\Omega \subset \mathbb{R}^3$, where anatomical structure is highly variable and prone to large registration errors due to being far away prostate surfaces used to perform the registration, we model the appearance of the prostate volume and the volume immediately outside the gland boundary. Using the whole gland prostate surface segmentation S_{MR}, we use morphological filtering to dilate the binary whole gland mask with a large circular filter to define this region, and we denote voxel locations within this volume $\mathbf{x} \in \Omega_P \subset \Omega$. For each MRI-TRUS image pair, we extract and vectorize the joint MRI-TRUS intensity appearance in this region $\mathbf{j}_i = [\mathbf{m}_i, \mathbf{u}_i]^T$, where $\mathbf{m}_i \in \mathbb{R}^d$ and $\mathbf{u}_i \in \mathbb{R}^d$ are the vectors of d voxel intensities in $I'_{\text{MR},i}(\mathbf{x})$ and $I'_{\text{TRUS},i}(\mathbf{x}), \forall \mathbf{x} \in \Omega_P$, respectively. The N joint appearance vectors are realizations of the distribution of MRI-TRUS joint intensity appearance $\mathcal{J}$ between the pre-procedure MRI and intra-procedure TRUS imaging. In this work, we model the distribution of deformations $\mathcal{J}$ and synthesize TRUS images using two methods: *(i)* a linear global appearance model using principal component analysis (PCA); and *(ii)* a non-linear global appearance model using dictionary learning.

Appearance modeling and synthesis using PCA PCA estimates the eigenvectors of $\mathcal{J}$'s covariance matrix

$$\mathbf{j} = \bar{\mathbf{j}} + \mathbf{\Phi}\mathbf{w} \tag{1}$$

where the eigenvectors $\mathbf{\Phi} = [\boldsymbol{\phi}_1, \ldots, \boldsymbol{\phi}_N] \in \mathbb{R}^{2d \times N}$ are the N principal modes of MRI-TRUS appearance, $\bar{\mathbf{j}}$ is the mean appearance for the training data, and $\mathbf{w} \in \mathbb{R}^N$ is a vector of eigenvectors weights. Figure 2 illustrates an example set of eigenvectors generated by our model. To synthesize the novel TRUS image, we first get the target MRI intensity vector $\mathbf{m}$, which contains the voxel intensities $I_{\text{MR}}(\mathbf{x}), \forall \mathbf{x} \in \Omega_P$. We then create the joint appearance vector as $\mathbf{j} = [\mathbf{m}, \mathbf{0}]^T$, where $\mathbf{0}$ is a zero vector that reflects the TRUS image that we want to synthesize. We perform the TRUS image synthesis operation by projecting $\mathbf{j}$ onto the appearance eigenvectors and solving for $\mathbf{w}$ in (1)

$$\hat{\mathbf{w}} = \mathbf{\Phi}^T(\mathbf{j} - \bar{\mathbf{j}}_m),$$

where we set the TRUS component of the mean appearance vector to zero $\bar{\mathbf{j}}_m = [\bar{\mathbf{m}}, \mathbf{0}]$, and then substitute this result back into (1)

$$\hat{\mathbf{j}} = \bar{\mathbf{j}} + \mathbf{\Phi}\hat{\mathbf{w}}. \tag{2}$$

The resulting joint appearance solution $\hat{\mathbf{j}} = [\hat{\mathbf{m}}, \hat{\mathbf{u}}]^T$ provides both the MRI reconstruction of minimum error $\hat{\mathbf{m}}$ with respect to the PCA model and the novel synthesized TRUS image in $\hat{\mathbf{u}}$.

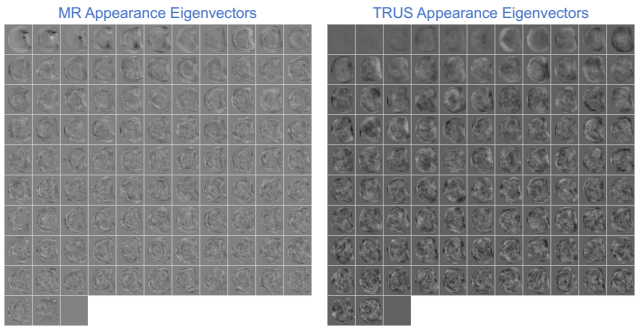

Fig. 2. Sample eigenvectors showing joint MRI-TRUS intensity appearance found using PCA. The joint eigenvector is the concatenation of the MRI eigenvector and the TRUS eigenvector at the same positions in the two corresponding matrices. The first principal component with the largest eigenvalue is shown in the top left corner and the remaining principal components are sorted in decreasing order of their eigenvalues from left to right and top to bottom.

Appearance modeling and synthesis using dictionary learning Dictionary learning, in comparison to PCA, provides a non-linear model of the distribution joint appearance $\mathcal{J}$. We use K-SVD to generate an overcomplete dictionary $\mathbf{D} = [\mathbf{d}_1, \ldots, \mathbf{d}_k] \in \mathbb{R}^{2d \times k}$ of K sparse joint appearance atoms [1]. While the atoms were created using the joint appearance vectors, each atom $k = 1, \ldots, K$ may be partitioned into separate MRI and TRUS components $\mathbf{d}_k = [\mathbf{d}_{\text{MR},k}, \mathbf{d}_{\text{TRUS},k},]^T$. Fig. 3 shows atoms from a sample dictionary of joint MRI-TRUS appearance. To reconstruct an MRI-TRUS appearance sample $\mathbf{j} = [\mathbf{m}, \mathbf{0}]^T$, where $\mathbf{0}$ is a zero vector that reflects the TRUS image that we want to synthesize, we solve the sparse coding problem

$$\hat{\boldsymbol{\gamma}} = \min_{\boldsymbol{\gamma}} \|\mathbf{j} - \mathbf{D}_m \boldsymbol{\gamma}\|_2^2 \quad \text{s.t.} \quad \|\boldsymbol{\gamma}\|_0 \leq \Gamma_0 \tag{3}$$

where $\mathbf{D}_m$ is the dictionary $\mathbf{D}$ with all K atoms having their TRUS appearance vectors set to zero $\mathbf{d}_{\text{TRUS},k} = \mathbf{0}$, $\boldsymbol{\gamma}$ is the sparse dictionary weighting coefficients, and Γ_0 is the dictionary's target sparsity constraint. We use orthogonal matching pursuit (OMP) to solve for (3). From (3), we have $\hat{\mathbf{j}} = \mathbf{D}\hat{\boldsymbol{\gamma}}$, where $\hat{\mathbf{j}} = [\hat{\mathbf{m}}, \hat{\mathbf{u}}]^T$ provides both the MRI reconstruction of minimum reconstruction error $\hat{\mathbf{m}}$ with respect to the dictionary model and the novel synthesized TRUS image in $\hat{\mathbf{u}}$.

3 Results and Discussion

From our database of $N = 105$ prostate biopsy patients, we perform leave-one-out testing. In each leave-one-out test, we selected the i-th patient's MRI as the reference image, and created a unique joint appearance model using the remaining $N - 1$ images as described in Sec. 2.2. For PCA-based modeling, we limited the model to use the first 3, 16, 46, and 102 eigenvectors, which corresponded

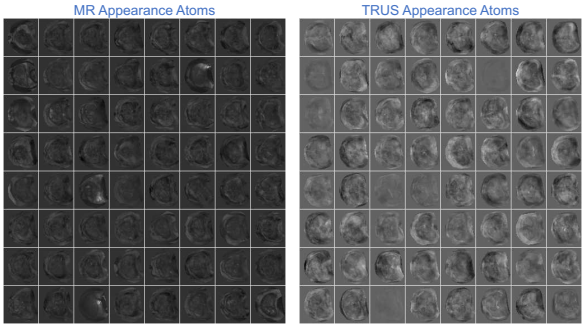

Fig. 3. Sample dictionary atoms showing joint MRI-TRUS intensity appearance found using K-SVD. The joint eigenvector is the concatenation of the MRI eigenvector and the TRUS eigenvector at the same positions in the two corresponding matrices.

to 50, 75, 90, and 100% of the model's cumulative variance, respectively. We also used the mean of the training TRUS images, which corresponded to using 0 eigenvectors in the PCA model, to synthesize the TRUS. For the dictionary learning-based model, we set our dictionary to have $K = 64$ atoms and a sparsity constraint $\Gamma_0 = 16$. All MR images were resampled to have 1.0 mm isotropic voxel spacing.

We evaluated TRUS image synthesis both qualitatively and quantitatively by comparing how similar the synthesized image was to patient i's corresponding target TRUS image. Fig. 4 shows example synthesized TRUS images and compares them to their respective target TRUS. These results show the synthesized TRUS images appearing more realistic as more eigenvalues are used in the PCA models. The synthesized TRUS appearance changes from the smooth mean TRUS appearance using 0 eigenvectors to gradually include more appearance details as more eigenvectors are used. The dictionary learning-based model synthesized TRUS images nearly identical in appearance to the PCA model using 102 eigenvectors, but did so using only 16 atoms, an 84% reduction in appearance dimensionality. Ideally, the synthesized TRUS and target TRUS images should exhibit similar structural appearance at corresponding locations, however we note that registration errors might still exists between the MRI and TRUS images since surface-based registration was used to align the datasets in Sec. 2.1. Fig. 4 also shows the reconstructed MRIs (created using the PCA-based model with 102 eigenvectors) for the example patients. These MRI reconstructions appear to capture the overall appearance of the original MRI, but omit some of the subtle anatomical features, for example the low intensity lesion at the bottom of subject 37's prostate.

Quantitatively, we calculated the correlation coefficient (CC) between the synthesized TRUS image and the target TRUS image, using only the voxels close to the prostate gland in Ω_P. Fig. 5 shows the distributions of CC values for the various appearance models. The mean CC values decreased as more eigenvectors were used for the PCA-based models, and the PCA-based model

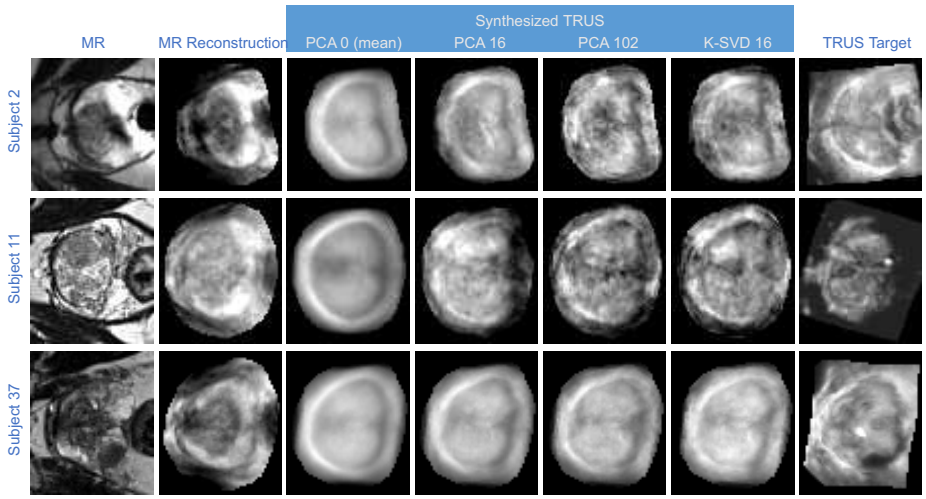

Fig. 4. Example MRI-TRUS image synthesis results from three subjects. From left to right, we show each patient's prostate MRI, the reconstructed MRI from the joint appearance model (using PCA 102), synthesized TRUS images found using both the PCA and dictionary learning (K-SVD) methods, and the patient's target TRUS image. Here, PCA X indicates that X eigenvectors were used for the synthesis, with PCA 0 indicating that the mean TRUS image. K-SVD 16 indicates a sparsity constraint of 16 atoms for the synthesis.

using 102 eigenvectors and dictionary learning model showed no significant differences (two-tailed, paired t-test, $p = 0.32$). All other combinations of methods compared gave significantly different similarity values (two-tailed, paired t-test, $p \leq 0.05$). These results appear to indicate that while the synthesized TRUS images in Fig. 4 appear more realistic, the structures synthesized do not actually correlate well with those in target TRUS. Interestingly, the smoothest synthetic TRUS images, those created using the mean intensity of the TRUS data (PCA 0) had the highest mean CC.

4 Conclusion

The method proposed in this paper can be used to create models of multi-modal image appearance, which in turn can be used to generate synthetic images of one modality from the other. Our results show that using a data-driven approach to image appearance modeling can both produce realistic MRI reconstructions and synthesize realistic TRUS images. We tested two different approaches to modeling MRI-TRUS appearance, using PCA and dictionary learning-based methods. Interestingly, the dictionary learning approach appears to provide similar qualitative and quantitative synthesis results compared to PCA, but does so with an 84% reduction in appearance dimensionality. For this preliminary study, we utilized a global approach to appearance synthesis. However, the results show that

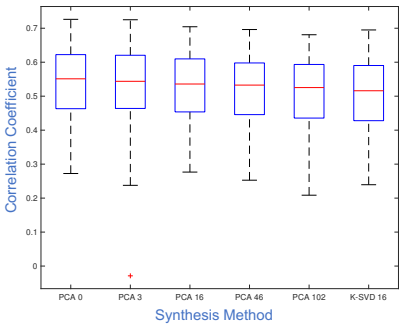

Fig. 5. Boxplots show the distribution of correlation coefficient similarity measures between synthesized TRUS images and their corresponding target TRUS image using different appearance model methods. Here, PCA X indicates that X eigenvectors were used for the synthesis, with PCA 0 indicating that the mean TRUS image. K-SVD 16 indicates a sparsity constraint of 16 atoms for the synthesis. Only PCA 102 and K-SVD 16 had no significant differences (two-tailed, paired t-test, $p = 0.32$), while all other method comparisons showed significant differences (two-tailed, paired t-test, $p \leq 0.05$)

such a global model of image appearance may not sufficiently capture the unique anatomical features present in the test images. Patch-based learning and synthesis methods may be better suited for learning such non-global appearances. In future work, we aim to explore using local, patch-based joint appearance modeling, and we envision that our global model of appearance presented in this work could serve as an initial pre-processing step prior to local appearance modeling and synthesis. Future work will also incorporate these synthetic TRUS images into the image registration process, and then quantifying target registration error of expertly identified matching landmarks identified in both the pre-procedure MRI and intra-procedure TRUS imaging to see how it compares with the current clinical standard that uses surface-based registration.

Acknowledgments and Disclosure

This work was supported in part by the NIH under grant R41/42-CA186414. Disclosure: Dr. Papademetris is a consultant for Electrical Geodesics, Inc.

References

1. Aharon, M., Elad, M., Bruckstein, A.: K -svd: An algorithm for designing overcomplete dictionaries for sparse representation. Signal Processing, IEEE Transactions on 54(11), 4311 –4322 (2006)
2. Barentsz, J.O., Richenberg, J., Clements, R., Choyke, P., Verma, S., Villeirs, G., Rouviere, O., Logager, V., Fütterer, J.J.: ESUR prostate MR guidelines 2012. European Radiology 22(4), 746–757 (2012)

3. Chui, H., Rangarajan, A.: A new point matching algorithm for non-rigid registration. Computer Vision and Image Understanding 89(2-3), 114 – 141 (2003)
4. Jog, A., Carass, A., Roy, S., Pham, D.L., Prince, J.L.: MR image synthesis by contrast learning on neighborhood ensembles. Medical image analysis 24(1), 63–76 (aug 2015)
5. Jog, A., Roy, S., Carass, A., Prince, J.L.: Magnetic resonance image synthesis through patch regression. IEEE 10th International Symposium on Biomedical Imaging (ISBI) 2013, 350–353 (2013)
6. Karnik, V.V., Fenster, A., Bax, J., Cool, D.W., Gardi, L., Gyacskov, I., Romagnoli, C., Ward, A.D.: Assessment of image registration accuracy in three-dimensional transrectal ultrasound guided prostate biopsy 37(2), 802–813 (2010)
7. Mitra, J., Mart, R., Oliver, A., Llad, X., Ghose, S., Vilanova, J., Meriaudeau, F.: Prostate multimodality image registration based on B-splines and quadrature local energy. Int. J. of Comp. Assisted Radiology and Surgery 7(3), 445–454 (2012)
8. Moradi, M., Janoos, F., Fedorov, A., Risholm, P., Kapur, T., Wolfsberger, L., Nguyen, P., Tempany, C., Wells, W.: Two solutions for registration of ultrasound to MRI for image-guided prostate interventions. In: IEEE EMBC. pp. 1129–1132 (2012)
9. Narayanan, R., Kurhanewicz, J., Shinohara, K., Crawford, E.D., Simoneau, A., Suri, J.: MRI-ultrasound registration for targeted prostate biopsy. In: IEEE ISBI. pp. 991–994 (2009)
10. Papademetris, X., Jackowski, A.P., Schultz, R.T., Staib, L.H., Duncan, J.S.: Computing 3D non-rigid brain registration using extended robust point matching for composite multisubject fMRI analysis. In: MICCAI, vol. 2879, pp. 788–795. Springer (2003)
11. Rueckert, D., Sonoda, L., Hayes, C., Hill, D., Leach, M., Hawkes, D.: Nonrigid registration using free-form deformations: application to breast MR images. IEEE TMI 18(8), 712 –721 (1999)
12. Sparks, R., Nicolas Bloch, B., Feleppa, E., Barratt, D., Moses, D., Ponsky, L., Madabhushi, A.: Multiattribute probabilistic prostate elastic registration (MAPPER): Application to fusion of ultrasound and magnetic resonance imaging. Medical Physics 42(3), 1153–1163 (2015)
13. Sun, Y., Yuan, J., Rajchl, M., Qiu, W., Romagnoli, C., Fenster, A.: Efficient Convex Optimization Approach to 3D Non-rigid MR-TRUS Registration. In: Mori, K., Sakuma, I., Sato, Y., Barillot, C., Navab, N. (eds.) Medical Image Computing and Computer-Assisted Intervention MICCAI 2013, Lecture Notes in Computer Science, vol. 8149, pp. 195–202. Springer Berlin Heidelberg (2013)
14. Tempany, C., Straus, S., Hata, N., Haker, S.: MR-guided prostate interventions. Journal of Magnetic Resonance Imaging 27(2), 356–367 (2008)
15. Ukimura, O., Faber, K., Gill, I.S.: Intraprostatic targeting. Current opinion in urology 22(2), 97–103 (2012)
16. Xu, S., Kruecker, J., Guion, P., Glossop, N., Neeman, Z., Choyke, P., Singh, A.K., Wood, B.J.: Closed-Loop Control in Fused MR-TRUS Image-Guided Prostate Biopsy. In: Ayache, N., Ourselin, S., Maeder, A. (eds.) Medical Image Computing and Computer-Assisted Intervention – MICCAI 2007, vol. 4791, pp. 128–135. Springer Berlin Heidelberg (2007)
17. Xu, S., Kruecker, J., Turkbey, B., Glossop, N., Singh, A.K., Choyke, P., Pinto, P., Wood, B.J.: Real-time MRI-TRUS fusion for guidance of targeted prostate biopsies. Computer Aided Surgery 13(5), 255–264 (2008)